J Therm Anal Calorim (2011) 103:319–327
DOI 10.1007/s10973-010-0961-z

Crystallization kinetics of poly(vinylidene fluoride)/MMT, SiO_2, $CaCO_3$, or PTFE nanocomposite by differential scanning calorimeter

Wenzhong Ma · Xiaolin Wang · Jun Zhang

Received: 20 January 2010 / Accepted: 8 July 2010 / Published online: 29 July 2010

Abstract The nonisothermal crystallization kinetics of poly(vinylidene fluoride) (PVDF) in PVDF/MMT, SiO_2, $CaCO_3$, or PTFE composites was investigated through differential scanning calorimetry measurements. The enhanced nucleation of PVDF in its nanocomposites with four types of nanoparticle, and their impact on the crystallization kinetics and melting behaviors were discussed. The modified Avrami method and combined Ozawa–Avrami approaches successfully described the primary crystallization of PVDF in nanocomposite samples under the nonisothermal crystallization process. The activation energy was determined according to the Friedman method and it was quite fit with the results of the analysis according to the modified Avrami model and a combined Ozawa–Avrami model.

Keywords Poly(vinylidene fluoride) (PVDF) · Nanocomposite · Nonisothermal crystallization · Differential scanning calorimetry (DSC)

Introduction

Over the last decade, increasing demand for special materials has led to the conception of composites. Nanoparticles in general, and nanoclays in particular, with their nanometer size, high surface area, and the associated predominance of interfaces in the nanocomposites, can function as structure and morphology directors [1]. Small amount addition of nanoclays or other nanoparticles into polymer products has been extensively utilized in an attempt to enhance the mechanical, thermal, optical, and physicochemical properties, especially enhancing modulus, strength, and heat resistance and reducing gas permeability and flammability compared to the pristine polymers. Poly(vinylidene fluoride) (PVDF), as a semi-crystalline polymer with excellent physical and chemical properties, as well as good thermal stability, has been widely used in many applications [2]. Similarly, many properties of PVDF are improved by an incorporation of nanofillers. The inclusion of ceramic particles in the PVDF polymer matrix increase the relative permittivity, the complex dielectric constant, and dynamical mechanical response of the composites [3, 4]. Especially, PVDF has its potential applications as piezoelectric and pyroelectric material, due to the presence of β crystalline phase. In order to enhance this crystalline phase formation, nanoclay was incorporated into PVDF matrix [5–7]. In recent years, some researchers have focused on the effects of nanosilica on the crystalline phase and the resulted material mechanical properties of this kind of nanacomposites [1, 8–10]. Shah et al. [1] have reported that in the case of the PVDF nanocomposites, the silicate layers leads to the β phase crystal, and these samples possess increased toughness due to the ability of nanoparticles to dissipate energy. They pointed that good nanoscale dispersion, coupled with favorable polymer–silicate interactions, is a critical factor. As demonstrated, Vo and Giannelis [11] used inorganic nanoparticles as an alternative means to control interfacial properties. Although so many research works have been devoted to the crystal structure and crystallization behaviors of PVDF and its nanocomposites, less

W. Ma · X. Wang (✉)
State Key Laboratory of Chemical Engineering, Department of Chemical Engineering, Tsinghua University, Beijing 100084, China
e-mail: xl-wang@tsinghua.edu.cn

J. Zhang
College of Materials Science and Engineering, Nanjing University of Technology, Nanjing 210009, China

attention has been paid to its nonisothermal crystallization kinetics.

Generally, studies of crystallization are limited to idealized conditions, in which external conditions are constant. In real situations, however, the external conditions change continuously, which make the treatment of nonisothermal crystallization more complex. The study of crystallization in a continuously changing environment is of greater interest, since industrial processes proceed generally under non-isothermal conditions [12]. Thermal analysis method such as differential scanning calorimetry (DSC), was widely applied to characterize the thermal behaviors of polymers, especially for the crystallization kinetics of crystalline polymers [13–17]. A better understanding about the relationship among processing, structure and properties of PVDF nanocomposites can be obtained if the kinetic of nonisothermal crystallization is studied under dynamical conditions. In Yu and his coauthors' work [18], the Avrami approach modified by Jeziorny successfully describe the nonisothermal crystallization process of PVDF/montmorillonite (MMT) composite with 2 wt% MMT. However, the effect of the nanoclay MMT content on the nonisothermal crystallization of PVDF nanocomposite has not been revealed clearly. In this work, the nonisothermal crystallization behaviors and nonisothermal crystallization kinetics of PVDF and PVDF/nanoparticles composites with various nanoparticle contents were discussed in detail.

Experimental

Materials

PVDF (Kynar K-761), in a powder form was supplied by Elf Atochem of North America Inc. (USA). Commercial grade of nanoparticles, such as montmorillonite clay (MMT with 24–26 Å silicate layers distance, organically modified with dimethyl dihydroenated tallow ammonium, Nanomer I.44P), was supplied by Nanocor (USA); silicon dioxide (SiO_2 with average size of about 20 nm, a high surface area fumed silica, which has been surface modified with hexamethyldisilazane, TS-530) was supplied by Cabot (USA); the powder of poly(tetrafluoroethylene) (PTFE with average size of about 500 nm, 7A–J) were purchased from Dupont (USA); and the inorganic nanoparticle of $CaCO_3$ with average size of about 100 nm is of industrial grade, which is bought directly from Omya (China). The nanoparticle size of SiO_2, $CaCO_3$, and PTFE were observed by SEM measurement, but that of MMT was given by the company directly.

Preparation of samples

The PVDF/nanoparticles composites were prepared with different types of nanoparticles by using a mini twin-screw extruder (ULTnano TW05, Technovel corporation, Japan) with various weight percentages (0.1, 1.0, 5.0 wt%) of each type of nanoparticles. The rate of screw was 120 rpm, the processing temperature of the extruder was set at 443, 473, 503, and 503 K from the hopper to the die, and the residence time was for 10 min.

Differential scanning calorimetry (DSC) measurement

Nonisothermal crystallization was carried out on a TA Instruments Q-200 differential scanning calorimeter in a dry nitrogen atmosphere. A sample of about 10 mg was heated up first to 473 K rapidly and kept for 3 min to eliminate the thermal history. Then, the sample was cooled down to 323 K at a cooling rate of 2.5, 5, 10, and 20 K min^{-1} with subsequently reheating to 473 K with the same heating rate of 10 K min^{-1}, respectively. The crystallinity of PVDF (X_c) was recorded below, as our previous work [19, 20].

Theory

Nonisothermal crystallization kinetics

Many of the approaches for describing the crystallization kinetics are based on the Avrami equation [21, 22]:

$$1 - X_t = \exp(-Z_t t^n), \tag{1}$$

$$\ln[-\ln(1 - X_t)] = n \ln t + \ln Z_t, \tag{2}$$

where X_t is the relative degree of crystallinity; the exponent n is a mechanism constant, the value of which depends on the type of nucleation and growth process parameters; the parameter Z_t is a composite rate constant involving nucleation and growth rate parameters.

Later, a number of workers tried to use it fit experimental results obtained from crystalline or semi-crystalline polymers, Jeziorny [23] pointed out that the parameter for value of rate Z_t, should be adequately corrected with the cooling rate D on which the nonisothermal crystallization depends:

$$\ln Z_c = \frac{\ln Z_t}{D}. \tag{3}$$

Ozawa [24] assumed that a nonisothermal process is the result of an infinite number of small isothermal steps according to Eq. 4:

$$1 - X_t = \exp\left[-\frac{K(T)}{D^m}\right] \quad (4)$$

where $K(T)$ is cooling function, m is the Ozawa exponent that depends on the dimension of the crystal growth. Combining the Avrami model Eq. 1 and Ozawa model Eq. 4 for nonisothermal polymer crystallization analysis, another form of the analysis model was induced by Liu and coworkers [25]:

$$\ln(D) = \ln F(T) - a \ln t, \quad (5)$$

where the parameter $F(T) = [K(T)/Z_t]^{1/m}$ refers to the value of cooling rate, which has to be chosen at unit crystallization time when the measured system amounts to a certain crystallinity; a is the ratio of the Avrami exponent n to the Ozawa exponent m, i.e., $a = n/m$.

Effective activation energy

From the variation of crystallization peak temperature (T_p) measured by DSC with the various cooling rates, Kissinger method [26] was widely used to estimate the activation energy ΔE. However, to drop the negative sign in cooling process may result in errors [27]. The differential isoconversional method of Friedman [28] and the advanced integral isoconversional method of Vyazovkin [29, 30] are appreciated to estimate the reliable values of the effective activation energy. The Friedman equation can be expressed as follows:

$$\ln\left(\frac{dX_t}{dt}\right)_{X_t} = \text{constant} - \frac{E_{X_t}}{RT_{X_t}}, \quad (6)$$

where dX_t/dt is the instantaneous crystallization rate as a function of time for a given value of the relative crystallinity (X_t), R the gas constant, and E_{X_t} the effective energy barrier of the process for a given value of X_t. At various cooling rates, a straight line can be obtained by plotting dX_t/dt versus $1/T_{X_t}$ and the slope is $-E_{X_t}/R$. Thus, the activation energy (E_{X_t}) can be calculated from the slope of the straight line.

Results and discussion

Effects of nanoparticles on the crystallization and melting behavior of PVDF

Figure 1A–D, cooling curves show a representative DSC scans of PVDF/nanoparticles composites with various nanoparticles contents, when cooling from 473 K at various rates. The melting curves show the subsequent melting behaviors for each cooling process at different cooling rates, which carried out at the same heating rate of 10 K min^{-1}.

For each samples (including the neat PVDF and composite samples), crystallization starts at higher temperatures when cooling rate is lower. Because cooling at a low rate, the melt polymer chains has enough response time to crystallize. While, at a higher cooling rate, the crystallization is finished in a shorter time and the activation of nuclei occurs at lower temperatures. This can be attributed to its longer period at lower viscosity temperature when polymer chains have greater mobility, easily arranging themselves to form more perfect crystallites [31]. As for the melting behavior, in each melt crystallization sample, the peak melting temperature is decreased with an increase of the cooling rate to some extent. When the cooling rate is increased, the polymer chains could not be correspondingly rearranged into the lattice in such a short time, leading to a lower melting peak temperature.

The nanoparticles type and their content dependence of the onset (T_c^{on}), peak (T_c^p), end (T_c^f), the difference between the onset and peak crystallization temperature (ΔT_c), melting enthalpy (ΔH_m) and the calculated crystallinity of PVDF (X_c) for PVDF in the PVDF/nanoparticles composites are shown in Table 1.

At a fixed cooling rate (2.5 K min^{-1}), for each PVDF nanocomposite system, the crystallization temperatures (including the values of T_c^{on}, T_c^p, T_c^f) of PVDF nanocomposite samples are higher than those of the neat PVDF. This indicates that the addition of these nanoparticles to PVDF matrix accelerated the nucleation of PVDF crystals. The small amount of nanoparticle addition ($\leq$1 wt%) mostly favors the crystallization of PVDF (Fig. 1), resulting in sharper crystallization peak and the lower value of ΔT_c. When the MMT, SiO_2, and PTFE content reaches to 5.0 wt%, the crystallization peak area is obviously smaller than that of the samples with $\leq$1.0 wt% addition of nanoparticles. This suggests that 1.0 wt% addition of these three types of nanoparticles remarkably enhance the nucleation of PVDF crystals. For the MMT composite sample, the value of melting enthalpy ΔH_m in 0.1 wt% MMT composite sample is very close to that of the neat PVDF sample. With an increase of the MMT content, ΔH_m is decreased in comparison with that of the neat PVDF sample (Table 1). This indicates that the enhanced nucleation of PVDF is reduced by more addition of MMT nanoparticles. Whereas with regards to $CaCO_3$ composite samples, the addition of 0.1–5.0 wt% would always accelerate the crystallization rate, leading to the narrower crystallization peak.

When the SiO_2, $CaCO_3$, and PTFE nanoparticles were incorporated into PVDF, the crystallinity of PVDF is increased with an increase of the nanoparticles addition. However, the MMT nanoparticles have less influence on the crystallinity of PVDF (Table 1). It is worth to note that when 1.0 wt% MMT is added into PVDF, the DSC scans

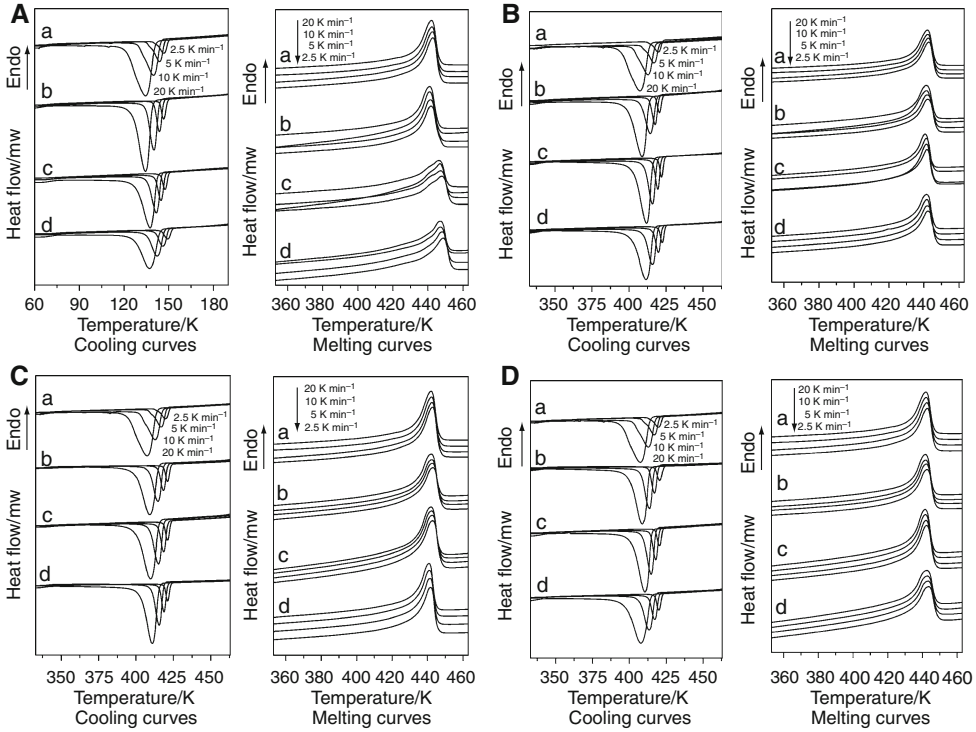

Fig. 1 DSC curves of nonisothermal crystallization at different cooling rates and those of melting behaviors at a heating rate of 10 K min^{-1} after nonisothermal crystallization for each PVDF/nanoparticles composite with various nanoparticle contents: **A** MMT; **B** SiO_2; **C** $CaCO_3$; **D** PTFE composite system; in each composite system: **a** neat PVDF; **b** 0.1 wt%; **c** 1.0 wt%; **d** 5.0%

Table 1 Characteristic data of nonisothermal melt crystallization behaviors for PVDF/nanoparticles composite samples crystallizing from the melt at 2.5 K min^{-1}

Nanoparticles content/wt%	T_c^{on}/K	T_c^{p}/K	T_c^{f}/K	ΔT_c/K	ΔH_m/J g^{-1}	X_c/%
PVDF-neat	422.8	419.6	414.3	3.2	37.3	35.7
MMT						
0.1	422.2	419.6	416.9	2.6	37.5	35.9
1.0	423.1	420.5	417.5	2.6	36.9	35.7
5.0	426.6	423.4	417.9	3.3	35.3	35.6
SiO_2						
0.1	422.9	420.6	417.8	2.3	42.0	40.2
1.0	423.9	422.0	419.7	1.9	38.7	37.4
5.0	424.5	422.5	419.9	2.0	37.6	37.9
$CaCO_3$						
0.1	423.3	421.1	418.5	2.2	37.3	35.7
1.0	423.3	421.2	418.5	2.1	38.8	37.5
5.0	423.2	421.2	418.9	2.0	37.7	38.0
PTFE						
0.1	423.4	420.6	417.3	2.8	42.4	40.6
1.0	422.7	420.6	417.5	2.1	40.7	39.3
5.0	422.5	420.0	417.3	2.5	38.0	38.3

D cool rate, T_c^{on} onset crystallization temperature of PVDF, T_c^{p} peak crystallization temperature of PVDF, T_c^{f} final crystallization temperature of PVDF, $\Delta T_c = T_c^{on} - T_c^{p}$, ΔH_m melting enthalpy, X_c crystallinity of PVDF

of the nanocomposite sample displayed two endotherms (Fig. 1A), but, when 5.0 wt% MMT was incorporated into PVDF, the lower temperature peak disappeared, and only the higher temperature peak remained. As reported, the two melting endotherms could be attributed to the melting of crystals with different morphologies [20, 32] or these crystals have different degrees of crystal perfection [33], and that these crystals can be melt and recrystalllize during DSC scans to yield more perfect crystals [21, 34]. In Fig. 1a, the two melting peaks are not influenced by the various cooling rate conditions, which indicates that recrystallization of PVDF during the heating process in DSC measurement may occur [35]. On the other hand, the MMT nanoparticles addition into PVDF could favor the formation of the β phase PVDF [6, 36]. The shifting of the PVDF melting peak also indicates a special interaction between PVDF chains and motmorillonite [6, 37]. Thorough identification of the double melting peaks in the MMT nanocomposite will be preceded in the future.

With regards to the melting curves of SiO_2, $CaCO_3$, and PTFE nanocomposites, only one melting peak is observed (Fig. 1B–D), which means that there is no recrystallization of PVDF during the DSC process or mixed crystal phase occurred during the crystallization in these nanocomposites. When 0.1 wt% nanoparticles was incorporated into PVDF (at 2.5 K min^{-1} heating rate), the crystallinity of PVDF is

Table 2 Nonisothermal crystallization kinetic parameters of the neat PVDF from Jeziorny model

Sample	D/K min^{-1}	Kinetic parameters			
		Z_c/min^{-1}	n	Adj. r^2	$t_{1/2}$/min
PVDF-neat	2.5	0.40	2.9	0.998	1.50
	5.0	0.79	3.5	0.999	0.87
	10	1.03	3.0	0.997	0.61
	20	1.10	3.4	0.999	0.40

Table 3 Nonisothermal crystallization kinetic parameters of PVDF/MMT nanocomposites from Jeziorny model

MMT content/wt%	D/K min^{-1}	Kinetic parameters			
		Z_c/min^{-1}	n	Adj. r^2	$t_{1/2}$/min
0.1	2.5	0.49	3.3	0.999	0.98
	5.0	0.87	3.8	0.999	0.54
	10	1.08	3.7	0.996	0.41
	20	1.15	4.1	0.998	0.33
1.0	2.5	0.47	3.3	0.999	1.28
	5.0	0.94	3.7	0.999	0.80
	10	1.13	3.8	0.996	0.56
	20	1.17	4.3	0.998	0.37
5.0	2.5	0.41	2.8	0.998	1.41
	5.0	0.87	3.1	0.999	0.80
	10	1.05	3.2	0.997	0.60
	20	1.10	3.4	0.999	0.40

increased from 35.7% of neat PVDF to 40.2%, 40.6% for SiO_2, and PTFE nanocomposite systems, respectively (Table 1). However, when the SiO_2 and PTFE content are higher than 1.0 wt%, the crystallinity of PVDF is reduced to some extent. The crystallization suppression is due to the restricted movement of the PVDF chains. Not only is the PVDF in smaller domains (such that the PVDF properties are no longer dominated by the larger and more bulklike domains), but the PVDF chains are constrained by clay platelets surrounding the domains [11]. As for $CaCO_3$ nanocomposite system, when 0.1 wt% $CaCO_3$ is added into PVDF, the crystallinity is not changed, but when more $CaCO_3$ addition leads to higher crystallinity of PVDF (Table 1). This means that less than 5.0 wt% $CaCO_3$ addition could always favor the crystallinity of PVDF.

Analysis of the nonisothermal crystallization of PVDF nanocomposites

Tables 2, 3, 4, 5, 6 show the kinetics parameters of nonisothermal crystallization in PVDF and its nanocomposite samples. The calculated values of n, Z_c, and the half crystallization time ($t_{1/2}$) obtained from the crystallization

Table 4 Nonisothermal crystallization kinetic parameters of PVDF/SiO_2 nanocomposites from Jeziorny model

SiO_2 content/wt%	D/K min^{-1}	Kinetic parameters			
		Z_c/min^{-1}	n	Adj. r^2	$t_{1/2}$/min
0.1	2.5	0.44	3.7	0.999	0.67
	5.0	0.92	3.7	0.999	0.44
	10	1.08	3.4	0.996	0.36
	20	1.11	3.9	0.993	0.26
1.0	2.5	0.47	3.4	0.998	0.59
	5.0	0.95	3.9	0.999	0.39
	10	1.14	3.9	0.999	0.30
	20	1.15	4.0	0.995	0.26
5.0	2.5	0.49	3.5	0.999	0.62
	5.0	0.95	3.6	0.999	0.44
	10	1.09	3.7	0.994	0.35
	20	1.14	3.7	0.998	0.27

Table 5 Nonisothermal crystallization kinetic parameters of PVDF/$CaCO_3$ nanocomposites from Jeziorny method

$CaCO_3$ content/wt%	D/K min^{-1}	Kinetic parameters			
		Z_c/min^{-1}	n	Adj. r^2	$t_{1/2}$/min
0.1	2.5	0.59	3.2	0.999	0.61
	5	0.95	3.5	0.999	0.44
	10	1.12	3.3	0.995	0.33
	20	1.12	3. 7	0.995	0.27
1.0	2.5	0.48	3.2	0.997	0.61
	5	0.92	3.4	0.997	0.43
	10	1.12	3.6	0.999	0.33
	20	1.13	4.0	0.998	0.26
5.0	2.5	0.49	3.4	0.998	0.60
	5	0.95	3.4	0.996	0.42
	10	0.97	3.9	0.996	0.29
	20	1.16	4.0	0.999	0.21

data are listed in these tables. In this work, the nonisothermal crystallization analysis is based on the primary crystallization stage. At the early state of crystallization, $\ln[-\ln(1 - X_t)]$ is in good linear relation with $\ln t$ (r^2 close to 1), which indicate that the modified Avrami equation is suitable for these systems. The Avrami exponent n of neat PVDF lies between 2.9 and 3.6 with various cooling rates, which is in agreement with Linares and his coworkers' work [38], and those four types of nanocomposite samples are around 3.0. This suggests that both the crystal growth of PVDF in the neat PVDF and PVDF nanocomposites should be a spherical three dimensional process.

In Tables 2, 3, 4, 5, 6, the values of Z_c (related to the overall crystallization rate [39]) is increased with an

Table 6 Nonisothermal crystallization kinetic parameters of PVDF/PTFE nanocomposites from Jeziorny model

PTFE content/wt%	D/K min^{-1}	Kinetic parameters			
		Z_c/min^{-1}	n	Adj. r^2	$t_{1/2}$/min
0.1	2.5	0.43	3.2	0.999	0.78
	5	0.88	3.9	0.999	0.43
	10	1.10	4.2	0.997	0.30
	20	1.16	3.9	0.999	0.24
1.0	2.5	0.49	3.1	0.997	0.66
	5	0.97	3.1	0.996	0.40
	10	1.14	3.5	0.996	0.30
	20	1.16	3.7	0.998	0.25
5.0	2.5	0.48	3.2	0.998	0.69
	5	0.91	3.5	0.999	0.47
	10	1.10	3.6	0.999	0.37
	20	1.10	3.4	0.997	0.30

increase of the cooling rate in each sample, which indicates that the crystallization rate of PVDF at a faster cooling rate is obviously higher than that at a slower cooling rate. At a fixed cooling rate, when 0.1–1.0 wt% MMT, SiO_2, and PTFE was incorporated into PVDF, the value of Z_c is gradually increased; while, when the composite has 5.0 wt% of these three types of nanoparticles, the value Z_c was decreased a little in comparison with that of 1.0 wt% addition composite. Similarly, the value $t_{1/2}$ also reflects the crystallization rate. The smaller this value, the more quickly the crystallization processed. It reveals that the 0.1–1.0 wt% of these four types of nanoparticles addition reduces the value $t_{1/2}$, but when the nanoparticles content is higher than 1.0 wt%, the value $t_{1/2}$ of the composite sample rises a little than that of 1.0 wt% composite samples. Therefore, less than 1.0 wt% nanoparticles addition can act as nucleating agents, leading to a higher crystallization rate than that of neat PVDF, but, when more addition is induced into PVDF, the crystallization would be hindered. It should be noted that when 0.1–5.0 wt% $CaCO_3$ is incorporated into PVDF, very close kinetics parameters of nonisothermal crystallization are obtained. Comparing with the neat PVDF sample, the value Z_c is higher, and $t_{1/2}$ is lower for $CaCO_3$ nanocomposites, which could infer that the $CaCO_3$ addition always accelerate the crystallization of PVDF. This result agrees with the crystallization and melting behaviors mentioned above.

Avrami analysis and its Jeziorny modification can describe only the primary stage of nonisothermal crystallization process of PVDF and its nanocomposite. In order to adequately describe the nonisothermal crystallization process, Mo et al. adopted a novel kinetic approach by combing the Avrami equation with the Ozawa equation [25]. According to Eq. 5, by plotting ln(D) vs. ln$t$, a series of lines at a given relative crystallinity can be produced (not shown). The results obtained from these lines for each nanocomposite systems are listed in Table 7, including the

Table 7 Nonisothermal crystallization kinetic parameters of PVDF/nanoparticles composites from combined Ozawa–Avrami method

X_t/%	20	40	60	80
PVDF-neat				
$F(T)$	4.0	6.4	9.5	14.6
a	1.7	1.7	1.7	1.7
MMT content/wt%				
0.1				
$F(T)$	3.2	4.8	6.6	9.5
a	1.8	1.8	1.9	2.0
1.0				
$F(T)$	2.9	4.5	6.5	10.2
a	1.8	1.8	2.0	2.2
5.0				
$F(T)$	3.5	5.7	8.5	12.9
a	1.8	1.8	1.8	1.9
SiO_2 content/wt%				
0.1				
$F(T)$	3.1	4.9	7.1	9.5
a	2.0	2.0	2.1	2.0
1.0				
$F(T)$	2.7	4.2	5.9	9.0
a	1.8	1.9	2.0	2.2
5.0				
$F(T)$	2.9	4.2	6.1	9.4
a	1.8	1.7	2.1	2.3
$CaCO_3$ content/wt%				
0.1				
$F(T)$	2.3	3.8	5.6	8.8
a	2.0	2.1	2.2	2.3
1.0				
$F(T)$	2.6	4.3	6.3	10.2
a	2.1	2.1	2.2	2.4
5.0				
$F(T)$	2.8	4.1	5.4	7.8
a	1.8	1.8	1.8	2.0
PTFE content/wt%				
0.1				
$F(T)$	3.5	5.1	6.8	9.5
a	1.6	1.6	1.6	1.7
1.0				
$F(T)$	2.7	4.0	5. 5	8.0
a	1.7	1.7	1.8	1.9
5.0				
$F(T)$	3.0	4.7	6.9	10.6
a	1.8	1.9	2.0	2.2

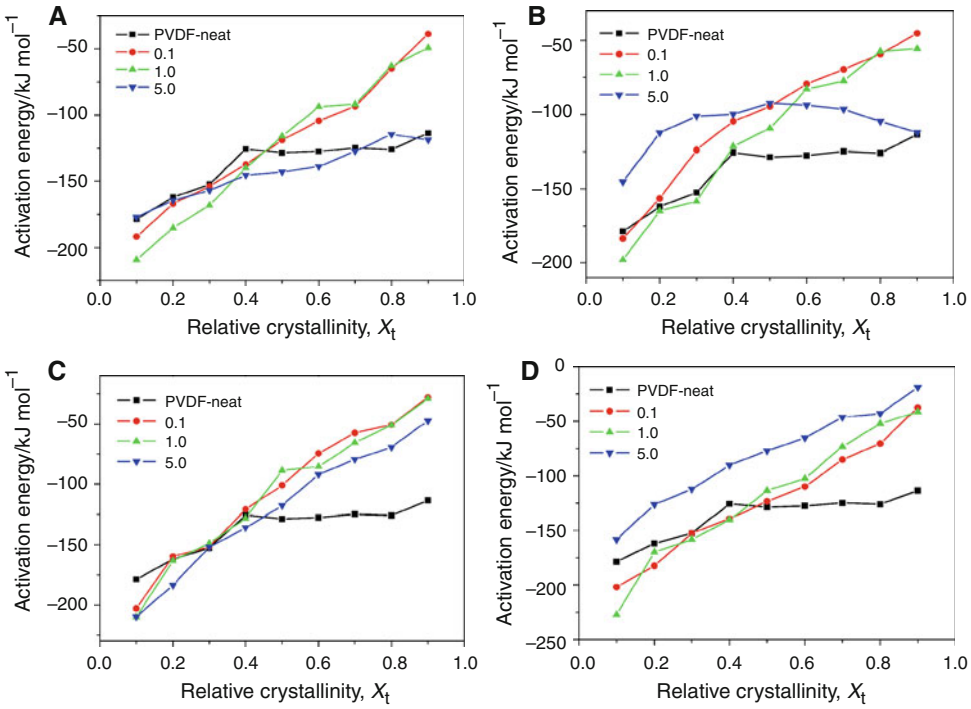

Fig. 2 Dependence of the effective activation energy on the relative crystallinity for each PVDF/nanoparticles composite: **A** MMT; **B** SiO_2; **C** $CaCO_3$; **D** PTFE composite system

kinetic parameter $F(T)$ and value of a ($=n/m$). $F(T)$ systematically increases with an increasing of the relative crystallinity, indicating that at a unit crystallization time, a higher cooling rate should be used to obtain a higher crystallinity [40]; but the values of a are almost constant for each sample, indicating the same spherical three-dimensional process. Comparing with the neat PVDF, at each value of X_t, the values of $F(T)$ for samples with these four types of nanoparticles addition are lower than those of neat PVDF, which means that the crystallization of PVDF is easier in these four system than that in the neat PVDF sample. When the MMT, SiO_2, and PTFE content is up to 5.0 wt%, the crystallization of PVDF is restricted to some extent, leading to a higher $F(T)$. These results are fitted well with the forth mentioned discussion. As for the $CaCO_3$ nanocomposite system, the values of $F(T)$ for samples with various contents of addition are very close but lower than those of neat PVDF. This indicates that the addition of $CaCO_3$ can favor the crystallization of PVDF.

The dependence of the effective activation energy on the relative crystallinity for these four nanocomposites based on Friedman equation is shown in Fig. 2. The activation energy is negative, which indicates the crystallization increases with decreasing temperature. It can be seen that the activation energy E_{X_t} increases with an increase of the relative crystallinity X_t (except of the 5.0 wt% SiO_2 nanocomposite sample), which means the crystallization becomes difficult with an increase of X_t. Comparing with the neat PVDF sample, at lower X_t (<40%), less than 1.0 wt% MMT, and PTFE nanocomposites show lower activation energy; however, at higher X_t, these composites showed higher activation energy. It could be ascribed to that these two types of nanoparticles acted as nucleating agents to facilitate the crystallization, however, hindered the crystallization at higher X_t. When these two types of nanoparticles content reaches to 5.0 wt%, the value of E_{X_t} is obviously higher than those containing less than 1.0 wt% nanoparticles, which means that the crystallization of PVDF in this sample is much more difficult in this condition. When 0.1–5.0 wt% $CaCO_3$ was added into PVDF, the effect on the effective activation energy is very similar. At lower X_t, $CaCO_3$ nanocomposites show lower activation energy; however, at higher X_t, these composites showed higher activation energy. It could be ascribed to that $CaCO_3$ nanoparticles acted as nucleating agents to facilitate the crystallization, however, hindered the crystallization at higher X_t. As demonstrated by Jeziorny and Mo methods, the addition of $CaCO_3$ particle also shows the similar influence on the crystallization. However, the trend in the SiO_2 composite samples is more complex (Fig. 2B). When the content of SiO_2 nanoparticles is 1.0 wt%, the nucleation effect is most remarkable, leading to the lower activation energy at lower X_t (<40%). When the content of SiO_2 nanoparticles is up to 5.0 wt%, the activation energy is a little declined at higher X_t. This trend is similar to the high density polyethylene/nanoscale calcium carbonate system, in which there is a change in crystallization mechanism [41].

Conclusions

In this work, the calculated kinetic parameters for series of MMT, SiO_2, $CaCO_3$, and PTFE nanocomposites were obtained from the DSC measurement. The results showed that the addition of MMT, SiO_2, and PTFE nanoparticles into PVDF matrix mainly influence early stage of the crystallization. As demonstrated by results of the kinetic approach by combining the Avrami equation with the Ozawa equation and the effective activation energy, the PVDF crystallization is favored by these nanoparticles addition with less than 1.0 wt%. When 5.0 wt% nanoparticle was added into PVDF, the crystallization of PVDF would be hindered to some extent. As for the $CaCO_3$ composite samples, the nucleating efficiency is always present in the composites. Even when 5.0 wt% $CaCO_3$ was added, the crystallization rate and effective activation are not reduced more. This suggests that the $CaCO_3$ particles are more effective to accelerate the crystallization of PVDF, especially for the early stage of crystallization.

Therefore, an understanding of the crystallization behaviors can help to develop an optimized processing condition for preparing PVDF/nanoparticles composites as engineering plastics with good properties.

Acknowledgements This work was supported by National Basic Research Program of China (2009CB623404), The National High Technology Research and Development Program of China-863 Program (2009AA062901), and Key-Project of Beijing Municipal Science & Technology Commission.

References

1. Shah D, Maiti P, Gunn E, Schmidt DF, Jiang DD, Batt CA, Giannelis EP. Dramatic enhancements in toughness of polyvinylidene fluoride nanocomposites via nanoclay-directed crystal structure and morphology. Adv Mater. 2004;16:1173–7.
2. Seiler DA. PVDF in the chemical process industry. In: Scheirs J, editor. Modern fluoropolymers. Chichester: Wiley; 1997. p. 487–505.
3. Mendes SF, Costa CM, Sencadas V, Nunes JS, Costa P, Gregorio R, Lanceros-Mendez S. Effect of the ceramic grain size and concentration on the dynamical mechanical and dielectric behavior of poly(vinilidene fluoride)/Pb(Zr0.53Ti0.47)O-3 composites. Appl Phys A Mater Sci Process. 2009;96:899–908.
4. Gregorio JR, Cestari M, Bernardino FE. Dielectric behaviour of thin films of beta-PVDF/PZT and beta-PVDF/$BaTiO_3$ composites. J Mater Sci. 1996;31:2925–30.
5. Pramoda KP, Mohamed A, Phang IY, Liu T. Crystal transformation and thermomechanical properties of poly(vinylidene fluoride)/clay nanocomposites. Polym Int. 2005;54:226–32.
6. Priya L, Jog JP. Poly(vinylidene fluoride)/clay nanocomposites prepared by melt intercalation: Crystallization and dynamic mechanical behavior studies. J Polym Sci B Polym Phys. 2002;40:1682–9.
7. Priya L, Jog JP. Polymorphism in intercalated poly(vinylidene fluoride)/clay nanocomposites. J Appl Polym Sci. 2003;89:2036–40.
8. Buckley J, Cebe P, Cherdack D, Crawford J, Ince BS, Jenkins M, Pan J, Reveley M, Washington N, Wolchover N. Nanocomposites of poly(vinylidene fluoride) with organically modified silicate. Polymer. 2006;47:2411–22.
9. Kim JW, Cho WJ, Ha CS. Morphology, crystalline structure, and properties of poly(vinylidene fluoride)/silica hybrid composites. J Polym Sci B Polym Phys. 2002;40:19–30.
10. Song R, Yang D, He L. Effect of surface modification of nanosilica on crystallization, thermal and mechanical properties of poly(vinylidene fluoride). J Mater Sci. 2007;42:8408–17.
11. Vo LT, Giannelis EP. Compatibilizing poly(vinylidene fluoride)/nylon-6 blends with nanoclay. Macromolecules. 2007;40:8271–6.
12. Ji GL, Zhu BK, Zhang CF, Xu YY. Nonisothermal crystallization kinetics of poly(vinylidene fluoride) in a poly(vinylidene fluoride)/dibutyl phthalate/di(2-ethylhexyl)phthalate system phase separation. J Appl Polym Sci. 2008;107:2109–17.
13. Zhang J, Chen SJ, Su J, Shi XM, Jin J, Wang XL, Xu ZZ. Non-isothermal crystallization kinetics and melting behavior of EAA with different acrylic acid content. J Therm Anal Calorim. 2009;97:959–67.
14. Zhang J, Chen SJ, Jin J, Shi XM, Wang XL, Xu ZZ. Non-isothermal melt crystallization kinetics for ethylene–acrylic acid copolymer in diluents via thermally induced phase separation. J Therm Anal Calorim. 2010. doi:10.1007/s10973-009-0619-x.
15. Achilias DS, Papageorgiou GZ, Karayannidis GP. Evaluation of the crystallisation kinetics of poly(propylene terephthalate) using DSC and polarized light microscopy. J Therm Anal Calorim. 2006;86:791–5.
16. Leszczynska A, Pielichowski K. Application of thermal analysis methods for characterization of polymer/montmorillonite nanocomposites. J Therm Anal Calorim. 2008;93:677–87.
17. Ying J, Liu S, Guo F, Zhou X, Xie X. Non-isothermal crystallization and crystalline structure of PP/POE blends. J Therm Anal Calorim. 2008;91:723–31.
18. Yu WX, Zhao ZD, Zheng WT, Long BH, Jiang Q, Li GW, Ji XW. Crystallization behavior of poly(vinylidene fluoride)/montmorillonite nanocomposite. Polym Eng Sci. 2009;49:491–8.
19. Ma WX, Zhang J, Chen SJ, Wang XL. Crystallization behavior and hydrophilicity of poly(vinylidene fluoride) (PVDF)/poly(styrene-co-acrylonitrile) (SAN) blend. Colloid Polym Sci. 2008;286:1193–202.
20. Ma WZ, Zhang J, Wang XL, Wang SM. Effect of PMMA on crystallization behavior and hydrophilicity of poly(vinylidene fluoride)/poly(methyl methacrylate) blend prepared in semi-dilute solutions. Appl Surf Sci. 2007;253:8377–88.
21. Avrami M. Kinetics of phase change. I. General theory. J Chem Phys. 1939;7:1103–12.
22. Avrami M. Kinetics of phase change. II. Transformation-time relations for random distribution of nuclei. J Chem Phys. 1940;8:212–24.
23. Jeziorny A. Parameters characterizing the kinetics of the non-isothermal crystallization of poly(ethylene terephthalate) determined by d.s.c. Polymer. 1978;19:1142–4.
24. Ozawa T. Kinetics of non-isothermal crystallization. Polymer. 1971;12:150–8.
25. Liu T, Mo Z, Wang S, Zhang H. Nonisothermal melt and cold crystallization kinetics of poly(aryl ether ether ketone ketone). Polym Eng Sci. 1997;37:568–75.
26. Kissinner HE. Variation of peak temperature with heating rate in different thermal analysis. J Res Natl Bur Stan. 1956;57:217–21.
27. Vyazovkin S. Is the Kissinger equation applicable to the processes that occur on cooling? Macromol Rapid Commun. 2002;23:771–5.
28. Friedman HL. Kinetics of thermal degradation of char-forming plastics from thermogravimetry. Application to a phenolic plastic. J Polym Sci C Polym Sympos. 1964;6:183–95.

29. Vyazovkin S, Sbirrazzuoli N. Isoconversional approach to evaluating the Hoffman–Lauritzen parameters (U* and Kg) from the overall rates of nonisothermal crystallization. Macromol Rapid Commun. 2004;25:733–8.
30. Vyazovkin S, Dranca I. Isoconversional analysis of combined melt and glass crystallization data. Macromol Chem Phys. 2006;207:20–5.
31. de Medeiros ES, Tocchetto RS, de Carvalho LH, Santos IMG, Souza AG. Nucleating effect and dynamic crystallization of a poly(propylene)/talc system. J Therm Anal Calorim. 2001;66: 523–31.
32. Ma WZ, Zhang J, Wang XL. Formation of poly(vinylidene fluoride) crystalline phases from the tetrahydrofuran/N, N-dimethylformamide mixed solvent. J Mater Sci. 2007;43:398–401.
33. Alamo R, Mandelkern L. Origins of endothermic peaks in differential scanning calorimetry. J Polym Sci B Polym Phys. 1986; 24:2087–105.
34. Marega C, Marigo A. Influence of annealing and chain defects on the melting behaviour of poly(vinylidene fluoride). Eur Polym J. 2003;39:1713–20.
35. Judovits L, Menczel JD, Leray AG. Molecular weight effects on the reorganization of poly(vinylidene fluoride), polyamide 12, and poly(p-phenylene sulfide). J Therm Anal Calorim. 1998;54: 605–22.
36. Priya L, Jog JP. Intercalated poly(vinylidene fluoride)/clay nanocomposites: structure and properties. J Polym Sci B Polym Phys. 2003;41:31–8.
37. Dillon DR, Tenneti KK, Li CY, Ko FK, Sics I, Hsiao BS. On the structure and morphology of polyvinylidene fluoride-nanoclay nanocomposites. Polymer. 2006;47:1678–88.
38. Linares A, Acosta JL, Martinez A, Garcí-Laureiro JI. Applications of a statistical model to the analysis of the kinetic parameters in isothermal and non-isothermal crystallization of polymer blends based on PVDF. Polymer. 1997;38:2741–6.
39. Di Lorenzo ML, Silvestre C. Non-isothermal crystallization of polymers. Prog Polym Sci. 1999;24:917–50.
40. Liu M, Zhao Q, Wang Y, Zhang C, Mo Z, Cao S. Melting behaviors, isothermal and non-isothermal crystallization kinetics of nylon 1212. Polymer. 2003;44:2537–45.
41. Huang JW, Wen YL, Kang CC, Tseng WJ, Yeh MY. Nonisothermal crystallization of high density polyethylene and nanoscale calcium carbonate composites. Polym Eng Sci. 2008;48:1268–78.